Investigation on Thermodynamic Properties of Ethanol + Gasoline Blended Fuel

ARTICLE *in* ENERGY & FUELS · JANUARY 2004

Impact Factor: 2.79 · DOI: 10.1021/ef030081v

3 AUTHORS, INCLUDING:

Zhaodong Nan
Yangzhou University
77 PUBLICATIONS **552** CITATIONS
SEE PROFILE

Zhi-Cheng Tan
Dalian Institute of Chemical Physics, Chinese…
323 PUBLICATIONS **2,768** CITATIONS
SEE PROFILE

Investigation on Thermodynamic Properties of Ethanol + Gasoline Blended Fuel

Zhaodong Nan,*,† Zhi-Cheng Tan,‡ and Lixian Sun‡

Department of Chemistry, Liaoning Normal University, Dalian 116029, People's Republic of China, and Thermochemistry Laboratory, Dalian Institute of Chemical Physics, Chinese Academy of Sciences, Dalian 116023, People's Republic of China

Received April 18, 2003

The heat capacities (C_p) of ethanol, unleaded gasoline 93# (where the "93" represents the octane number), and gasohol (which consisted of 10 wt % ethanol and 90 wt % unleaded gasoline 93#) were measured by adiabatic calorimetry in the temperature range of 80−320 K. For the gasoline, a glass−liquid transition was found at 92.42 K; for the gasohol, a glass−crystal transition and a solid−liquid transition were observed, at 93.17 and 150.86 K, respectively. The enthalpy and entropy of all of the transitions were derived based on the C_p data. For the gasoline, the enthalpy and entropy of the glass-liquid transitions were determined to be 6.80 J g^{-1} and 0.0736 J K^{-1} g^{-1}, respectively; for the gasohol, the enthalpy and entropy of the glass−crystal transition were determined to be 9.93 J g^{-1} and 0.107 J K^{-1} g^{-1} , respectively, and the enthalpy and entropy of the solid−liquid phase transition were determined to be 9.99 J g^{-1} and 0.0662 J K^{-1} g^{-1}, respectively. The polynomial equations of C_p, with respect to the thermodynamic temperature T, were established through the least-squares fitting. According to the thermodynamic relationship and the equations, the thermodynamic functions of the gasoline and the gasohol, and the excess thermodynamic functions of the gasohol, were derived.

1. Introduction

Nations today often face divergent challenges in the form of climate change, air pollution, energy production, consumption security, and shrinking oil supplies. In response to these challenges, countries around the world have developed programs to support the use of clean fuels, including ethanol.[1] The Chinese State Economic and Trade Commission required Sino-Petroleum Company (SINOPEC) to submit a feasibility report and make the production of ethanol-blended gasoline possible.[2] Gasoline will be replaced by an ethanol−gasoline blend (gasohol) for automobiles in China in the future.

Gasohol, as a fuel for automobiles, has been extensively studied.[3−15] This type of fuel can reduce greenhouse gas emissions and enhance the octane number of gasoline. However, to the best of our knowledge, the thermodynamic properties of gasohol have not been reported until recently. The thermodynamic properties of gasohol are necessary as the basic thermodynamic data for the investigation of clean fuels.

In this paper, the heat capacities (C_p) of the two systems—unleaded gasoline 93# (where the "93" represents the octane number) and gasohol that consisted of 10 wt % ethanol and 90 wt % unleaded gasoline 93#—were measured by an adiabatic calorimeter. The glass-transition temperatures and the phase-transition temperature of the two systems were determined. At the same time, the thermodynamic functions of the two systems were derived.

2. Experimental Section

The ethanol, which had a purity of >99.8%, was purchased from Shenyang Chemical Agent Factory. Unleaded gasoline 93#, which was used for calorimetric study, was purchased from the Dalian Branched Company of SINOPEC.

* Author to whom correspondence should be addressed. E-mail: zdnan65@hotmail.com.
† Liaoning Normal University.
‡ Dalian Institute of Chemical Physics.

(1) Vyas, S. In *Biomass: A Growth Opportunity in Green Energy and Value-Added Products*; Overend, R. P., Chornet, E., Eds.; Proceedings of the Fourth Biomass Conference of the Americas; Pergamon Press: New York, 1999; Vol. 2, pp 1725−1730.
(2) Zou, S. *China Pet. Process. Petrochem. Technol.* **2001**, *2*, 1−4.
(3) Hsieh, W. D.; Chen, R. H.; Wu, T. L.; Lin, T. H. *Atmos. Environ.* **2002**, *36*, (3), 403−410.
(4) Masuzo, Y. *Baiomasu Enerugi Riyo no Saishin Gijutsu*; Yukawa, H., Ed.; Shi Emu Shi: Tokyo, Japan, 2001; pp 287−297.
(5) Kremer, F. G.; Fachetti, A. *Soc. Automot. Eng.* **2001**, 1−4.
(6) Wang, M.; Saricks, C.; Wu, M. J. *Air Waste Manage. Assoc.* **1999**, *49*, (7), 756−772.
(7) Whitten, G. Z. *Environ. Sci. Technol.* **1998**, *32*, (23), 3840−3841.
(8) Tsai, H. H. *Shiyou Jikan* **1997**, *33*, (4), 71−82.
(9) Jones, B. E.; Ready, K. L.; Karges, M. A.; Willette, P. R. *Energy, Environment, Agriculture, and Industry*; Proceedings, Second Biomass Conference of the Americas; National Renewable Energy Laboratory: Golden, CO, 1995; pp 986−995.
(10) Kadakia, A. M.; Singh, S. N. *CEW, Chem. Eng. World* **1997**, *32*, (1), 71−76.
(11) Wyman, C. E. *Proceedings of the 2nd European Motor Biofuels Forum*; Joanneum Research Forschungsgesellschaft: Graz, Austria, 1996; pp 81−85.
(12) Galbe, M.; Larsson, M.; Stenberg, K.; Tengborg, C.; Zacchi, G. In *Fuels and Chemicals from Biomass*; Saha, B. C., Woodward, J., Ed.; ACS Symposium Series 666; American Chemical Society: Washington, DC, 1997; pp 110−129.
(13) Kremer, F. G.; Jardim, J. L. F.; Maia, D. M. *Soc. Automot. Eng. [Spec. Publ.] SP* **1996**, *SP-1208*, 415−422.
(14) Allsup, J. R.; Eccleston, D. B. *Proceedings of the International Symposium on Alcohol Fuels Technology, 3rd*, 1979; pp 1−7.
(15) Allsup, J. R.; Eccleston, D. B. *Energy Res. Abstr.* **1979**, *4*, (14), 2−17.

10.1021/ef030081v CCC: $27.50
Published on Web 11/13/2003

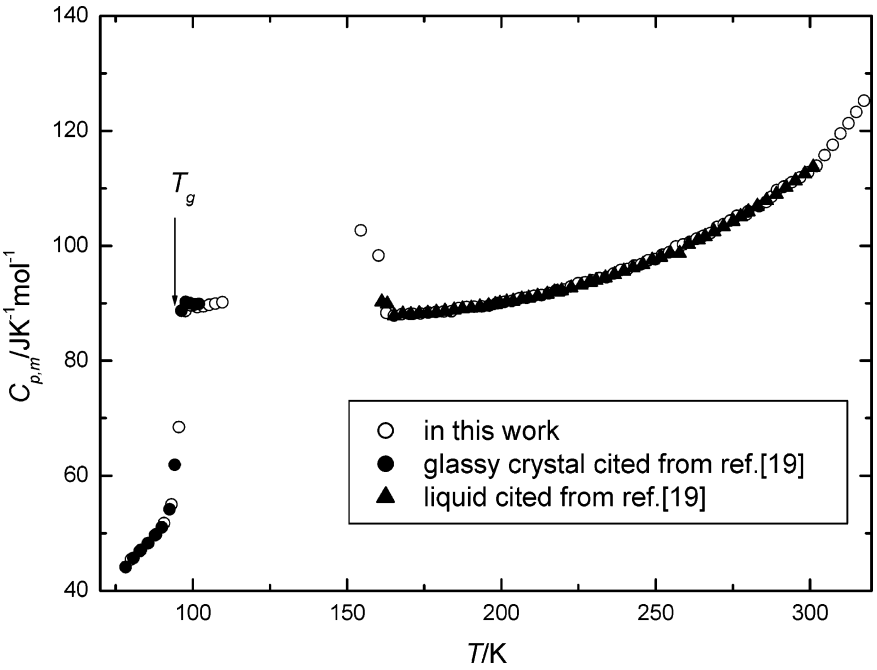

Figure 1. Experimental molar heat capacities of ethanol.

Table 1. Experimental Heat Capacities of the Unleaded Gasoline 93#

T (K)	C_p (J K^{-1} g^{-1})	T (K)	C_p (J K^{-1} g^{-1})	T (K)	C_p (J K^{-1} g^{-1})
83.32	0.92	148.50	1.81	232.01	1.93
84.95	0.93	150.36	1.81	234.56	1.94
86.96	0.97	152.21	1.80	237.08	1.94
88.92	1.04	154.06	1.80	239.57	1.95
90.78	1.18	155.91	1.81	242.02	1.95
92.42	1.44	157.76	1.80	244.50	1.96
93.86	1.65	159.61	1.79	247.01	1.96
95.19	1.75	161.46	1.79	249.53	1.96
96.52	1.76	163.31	1.80	252.03	1.97
97.83	1.74	165.14	1.81	254.52	1.98
99.14	1.75	166.98	1.81	257.02	1.99
100.45	1.77	168.82	1.80	259.49	2.00
101.77	1.75	170.65	1.81	261.97	2.01
103.09	1.73	172.48	1.81	264.44	2.01
104.42	1.74	174.31	1.79	266.89	2.03
106.10	1.75	176.12	1.81	269.34	2.05
108.09	1.75	177.94	1.83	271.79	2.05
110.08	1.76	179.76	1.82	274.22	2.05
112.07	1.75	182.02	1.83	276.66	2.07
114.06	1.74	184.73	1.83	279.08	2.07
116.05	1.76	187.43	1.83	281.51	2.09
118.03	1.76	190.13	1.83	283.93	2.08
119.98	1.77	192.82	1.83	286.33	2.08
121.93	1.77	195.49	1.84	288.74	2.09
123.85	1.77	198.15	1.86	291.13	2.10
125.78	1.79	200.82	1.87	293.50	2.13
127.70	1.78	203.47	1.87	295.87	2.13
129.60	1.78	206.11	1.87	298.23	2.15
131.51	1.77	208.75	1.89	300.58	2.16
133.40	1.78	211.37	1.89	302.93	2.15
135.32	1.76	213.99	1.90	305.26	2.18
137.23	1.77	216.60	1.90	307.59	2.19
139.13	1.77	219.19	1.89	309.92	2.17
141.01	1.77	221.77	1.90	312.23	2.18
142.89	1.78	224.36	1.91	314.53	2.22
144.76	1.78	226.92	1.92	316.84	2.22
146.63	1.80	229.46	1.92		

C_p measurements were performed in a high-precision automatic adiabatic calorimeter; the structure and procedure of the apparatus were described in detail elsewhere.[16,17] The principle of the calorimeter is based on the Nernst stepwise heating method. The calorimeter mainly consists of a sample cell, an adiabatic (or inner) shield, a guard (outer) shield, a platinum resistance thermometer, an electric heater, two sets of chromel-copel thermocouples, and a high-vacuum can. The sample cell was made of gold-plated copper with an inner volume of 48 cm^3. Eight gold-plated copper vanes with a thickness of 0.2 mm were put into the cell to promote heat distribution between the sample and the cell. The platinum resistance thermometer was inserted into the copper sheath, which was soldered in the middle of the sample cell. The heater wire was wound on the surface of the thermometer. The evacuated can was kept within a pressure of ca. 1×10^{-3} Pa during the C_p measurements, to eliminate the heat loss due to gas convection. Liquid nitrogen was used as the cooling medium. One set of six junctions of chromel-copel thermocouples was used to detect the temperature difference between the sample cell and the inner shield. Similarly, the other set of thermocouples was installed between the inner and outer shields. The temperature difference between them was maintained at 0.5 mK during the entire experimental process. The sample cell was heated by the standard discrete heating method. The temperature of the cell was alternatively measured. The temperature increment in a heating period was 2−4 K, and temperature drift was maintained at $\sim 10^{-3}$ K min^{-1} in an equilibrium period. All the calorimetric data were automatically recorded through a Data Acquisition/Switch Unit (model 34970A, Aglient, USA) and processed online by a computer.

To verify the reliability of the adiabatic calorimeter, the molar heat capacity for the reference standard material (α-Al_2O_3) was determined with the adiabatic calorimeter. The deviations of our experimental results from the recommended values of the former National Bureau of Standards (NBS)[18] were within ±0.2% in the temperature range of 80−400 K.

The masses of the ethanol, unleaded gasoline 93#, and gasohol used for C_p measurements were 13.1940, 13.0436, and 13.0416 g, respectively.

(16) Tan, Z. C.; Sun, G. Y.; Sun, Y.; Yin, A. X.; Wang, W. B.; Ye, J. C.; Zhou, L. X. *J. Therm. Anal.* **1995**, *45*, 59−67.

(17) Tan, Z. C.; Zhou, L. X.; Chen, S. X.; Yin, A. X.; Sun, Y.; Ye, J. C.; Wang, X. K. *Sci. Sin., Ser. B* **1983**, *26*, 1014−1026.

(18) Ditmars, D. A.; Ishihara, S.; Chang, S. S.; Bernstein, G.; West, E. D. *J. Res. Natl. Bur. Stand.* **1982**, *87*, 159−174.

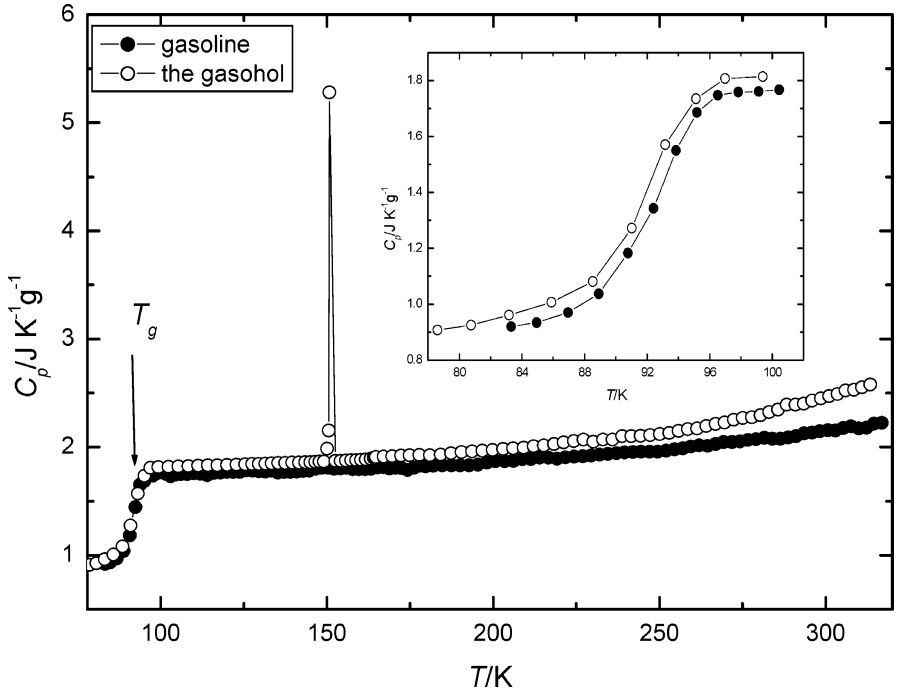

Figure 2. Experimental heat capacities of the unleaded gasoline 93# and the gasohol. Inset shows the glass transition of the unleaded gasoline 93# and the gasohol.

Table 2. Experimental Heat Capacities of the Gasohol

T (K)	C_p (J K^{-1} g^{-1})	T (K)	C_p (J K^{-1} g^{-1})	T (K)	C_p (J K^{-1} g^{-1})
80.76	0.93	150.86	5.28	235.92	2.07
83.19	0.96	152.55	1.87	238.77	2.10
85.90	1.01	154.17	1.87	241.55	2.10
88.54	1.08	155.74	1.88	244.36	2.10
91.03	1.27	157.27	1.88	247.23	2.11
93.17	1.57	158.79	1.88	250.08	2.12
95.13	1.74	160.26	1.88	252.92	2.13
97.00	1.81	161.71	1.88	255.73	2.15
99.40	1.81	163.13	1.89	258.55	2.17
102.36	1.82	164.79	1.91	261.33	2.17
105.39	1.82	167.10	1.91	264.11	2.19
108.38	1.83	169.72	1.92	266.87	2.22
111.26	1.83	172.33	1.92	269.61	2.23
114.23	1.83	174.94	1.93	272.32	2.25
117.11	1.83	177.84	1.93	275.04	2.27
119.96	1.83	181.02	1.92	277.73	2.28
122.80	1.84	184.19	1.93	280.40	2.30
125.43	1.84	187.35	1.94	283.06	2.32
127.58	1.84	190.50	1.95	285.68	2.35
129.57	1.85	193.64	1.96	288.27	2.39
131.50	1.85	196.76	1.97	290.84	2.39
133.42	1.85	199.87	1.97	293.40	2.40
135.40	1.85	202.96	1.98	295.95	2.43
137.49	1.85	206.04	1.99	298.48	2.45
139.60	1.86	209.11	2.00	301.02	2.47
141.61	1.86	212.17	2.01	303.52	2.49
143.43	1.86	215.21	2.01	305.98	2.52
145.07	1.86	218.23	2.03	308.44	2.53
146.49	1.86	221.24	2.05	310.90	2.55
147.77	1.87	224.24	2.06	313.36	2.58
149.18	1.87	227.18	2.07	315.81	2.57
150.06	1.99	230.10	2.05	318.19	2.60
150.62	2.15	233.02	2.07		

3. Results and Discussion

3.1. Determination of Heat Capacity. The C_p values of the ethanol, the unleaded gasoline 93#, and the gasohol were determined using an adiabatic calorimeter in the temperature range of 80−320 K. The results of the C_p measurements of the ethanol, as well as those for the unleaded gasoline 93# and the gasohol, are shown in Figures 1 and 2, respectively; the data for the unleaded gasoline 93# and the gasohol are listed in Tables 1 and 2, respectively. To compare the results of the C_p measurements for ethanol measured in our laboratory with those reported in the literature, the C_p data gained from the literature[19] are also given in Figure 1. This figure shows that the molar heat capacities reported in this paper are in excellent agreement with the data cited from ref 19. The glass-transition phenomenon was observed at a glass-transition temperature of $T_g = 97.46$ K, and through complex thermal behavior from 110 K to ~150 K, the sample finally was transformed to a stable crystal and melted at a melting temperature of $T_m = 158.94$ K. The values reported in ref 19 were determined to be $T_g = 97$ K and $T_m = 159.00 \pm 0.006$ K, respectively.

Figure 2 shows the variation in the heat capacities of the two systems, relative to increasing temperature. The plot of the heat capacity versus the temperature presents smooth curves in the temperature range of 96−320 K for the unleaded gasoline 93# and the ranges of 100−150 K and 160−320 K for the gasohol. In other words, no thermal anomalies were observed in these temperature ranges.

The C_p values of the two systems were fitted to the following polynomial expressions by the least-squares method:

(1) For the unleaded gasoline 93#, in the temperature range of 96−320 K,

$$C_p\,(\text{J K}^{-1}\,\text{g}^{-1}) = 1.025 \times 10^{-3}T^2 + 2.082 \times 10^{-3}T + 1.201 \quad (1)$$

where the correlation coefficient of the fitting is $R^2 = 0.9942$.

(19) Haida, O.; Suga, H.; Seki, S. *J. Chem. Thermodyn.* **1977**, *9*, 1133−1148.

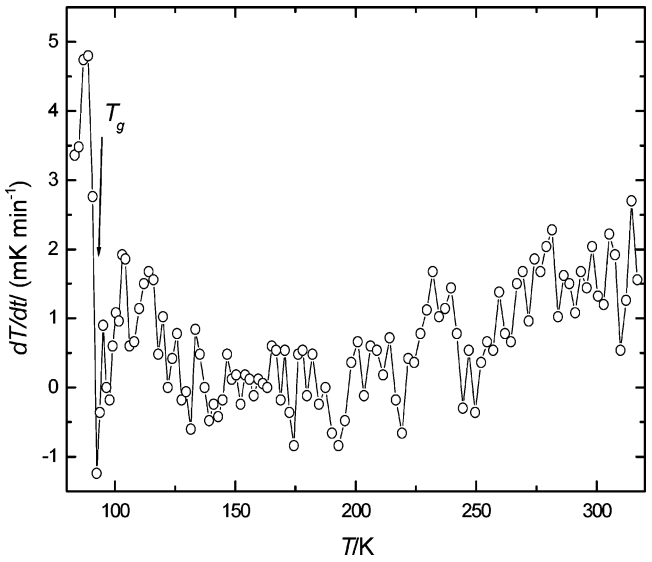

Figure 3. Temperature drift rates during heat-capacity (C_p) measurements of the unleaded gasoline 93#.

(2) For gasohol in the temperature range of 100−150 K,

$$C_p\ (\mathrm{J\ K^{-1}\ g^{-1}}) = 1.024 \times 10^{-3}T + 1.713 \qquad (2)$$

where $R^2 = 0.9966$.

(3) For gasohol in the temperature range of 160−320 K,

$$C_p\ (\mathrm{J\ K^{-1}\ g^{-1}}) = 2.116 \times 10^{-3}T^2 + 4.420 \times 10^{-3}T + 0.525 \qquad (3)$$

where $R^2 = 0.9944$.

3.2. Glass Transition and Phase Transition. Figure 2 shows that the heat capacities of the two systems clearly increase as the temperature increases in the region of 80−100 K. The inset in Figure 2 shows the change of the heat capacities clearly. The C_p value clearly changes before and after the glass-transition temperature (T_g).[20] Glass transitions then occur in the gasoline and gasohol systems in the temperature range of 80−100 K, as is the case for ethanol. The curves of the temperature drift rates during the C_p measurements in the two systems are shown in Figures 3 and 4, for the unleaded gasoline 93# and gasohol, respectively. These figures show that the temperature drift rates become larger during the glass transition. This is excellent agreement with the literature.[21,22] The temperature drift rates are less than ±2 mK min^{-1} at all temperatures except that of the phase transition for the gasohol, which shows that the adiabatic conditions are better. Thus, the experimental results are accurate and reliable. By analyzing the curves of dC_p/dT, with respect to T, the glass-transition temperatures of the two systems were determined to be $T_g = 92.42$ K for the unleaded gasoline 93# and $T_g = 93.17$ K for the gasohol. These temperatures correspond to those at which the values of dC_p/dT reach the maximum.

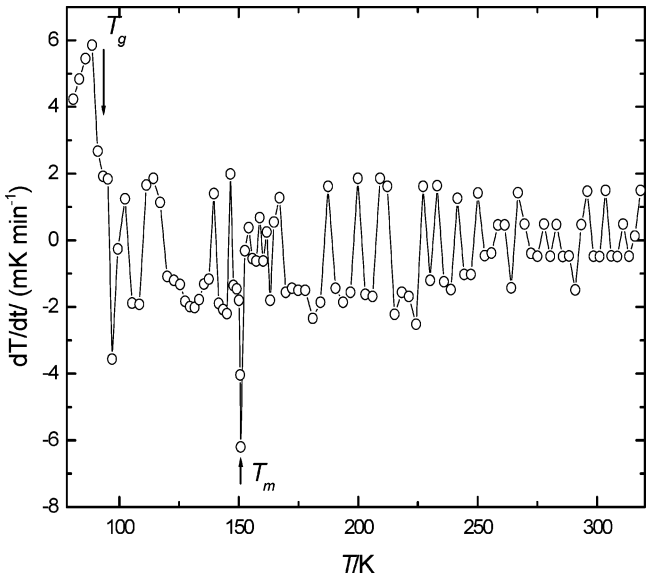

Figure 4. Temperature drift rates during C_p measurements of the gasohol.

No phase transition was observed for the unleaded gasoline 93# after the glass transition, which shows that the glassy structure of the unleaded gasoline 93# transformed directly to that of the liquid phase at the glass-transition temperature. However, for the gasohol, the C_p value reaches the maximum at 150.86 K, as observed in Figure 2. In other words, the solid−liquid phase transition was observed at this temperature. At the glass-transition temperature ($T_g = 93.17$ K), the glassy structure changes to a crystalline structure for the gasohol.

The glass-transition temperature of the gasohol ($T_g = 93.17$ K) is greater than that of the gasoline ($T_g = 92.42$ K) and is less than that of ethanol ($T_g = 97.46$ K). The reason may be that the glass-transition temperature can be affected by the structure change of the system. The hydrogen bond was formed by adding ethanol into the gasoline in the system. The glass-transition temperature increases when the molecular structure becomes more rigid, which is due to the increased number of polar groups.[24] The amount of polar groups (hydroxyl, −OH) of the system increases as ethanol is added into the gasoline. Thus, the glass-transition temperature of the gasohol is greater than that of the unleaded gasoline 93#. The content of ethanol in the gasohol is only 10 wt %; therefore, the glass-transition temperature of the gasohol is more similar to that of the unleaded gasoline 93#. The solid−liquid phase-transition enthalpy of the gasohol was calculated to be 9.99 J g^{-1}, which is equal to the melting enthalpy of the ethanol in the gasohol. The value of the phase-transition enthalpy of the gasohol is slightly less than that of the melting enthalpy 0.1 g ethanol, because the melting enthalpy of pure ethanol is 107.03 J g^{-1}.[19] The melting temperature of the gasohol (150.86 K) is less than that of ethanol, which is 159.00 K.[19] This means that the phase-transition enthalpy and the melting temperature of the gasohol were affected by the liquid

(20) Liu, Z. H.; Hatakeyama, T. *Handbook of Analytical Chemistry*, 2nd ed.; Chemical Industry Press: Beijing, 2000; p 64.

(21) Tsukushi, I.; Yamamuro, O.; Ohta, T.; Matsuo, T.; Nakano, H.; Shirota, Y. *J. Phys.: Condens. Matter* **1996**, *8*, 245−255.

(22) Suga, H. *J. Chim. Phys. Phys.−Chim. Biol.* **1985**, *82*, 275−289.

(23) Tan, Z. C.; Xue, B.; Lu, S. W.; Meng, S. H.; Yuan, X. H.; Song, Y. J. *J. Therm. Anal. Calorim.* **2001**, *63*, 297−308.

(24) Masson, J.-F.; Polomark, G. M.; Collins, P. *Energy Fuels* **2002**, *16*, 470−476.

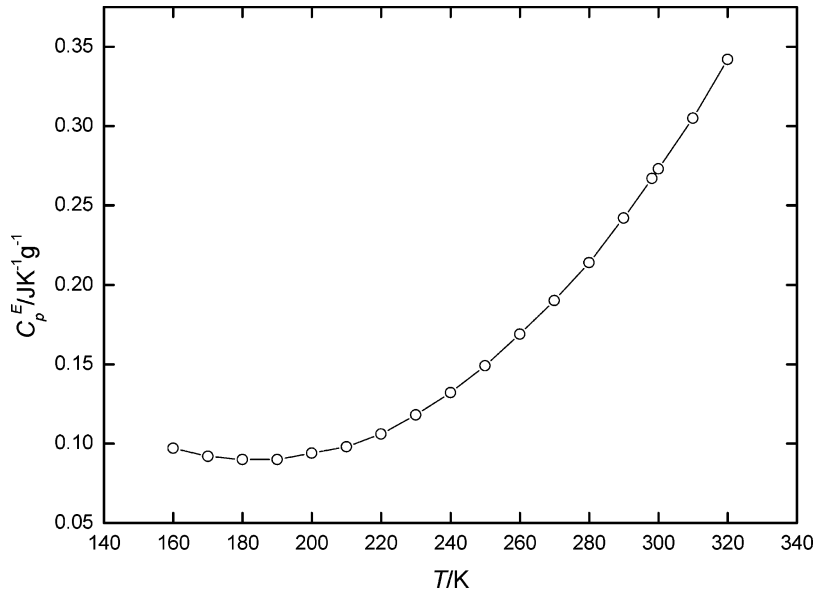

Figure 5. Excess heat capacities (C_p^E) of the gasohol.

gasoline. This may be ascribed to the fact that the amount of hydrogen bonds in the gasohol system is less than that in a pure ethanol system.

3.3. Enthalpy and Entropy of the Glass Transition and the Phase Transition. The enthalpy ($\Delta_g H$) and entropy ($\Delta_g S$) of the glass transition of the two systems were calculated according to the following relationships:

$$\Delta_g H = \frac{Q - q - m\int_{T_1}^{T_2} C_p \, dT}{m} \quad (4)$$

$$\Delta_g S = \frac{\Delta_g H}{T_g} \quad (5)$$

where Q is the total amount of heat introduced into the sample cell; q is the heat absorbed by the cell; m is the amount of mass of the sample; T_g is the glass-transition temperature; and T_1 and T_2 are the initial and final temperatures of the glass transition, respectively. For the unleaded gasoline 93#, $\Delta_g H = 6.80$ J g^{-1} and $\Delta_g S = 0.0736$ J K^{-1} g^{-1}; for the gasohol, $\Delta_g H = 9.93$ J g^{-1} and $\Delta_g S = 0.107$ J K^{-1} g^{-1}.

The melting enthalpy ($\Delta_m H$) and entropy ($\Delta_m S$) of the gasohol were calculated according to the following relationships:[23]

$$\Delta_m H = \frac{Q - m\int_{T_1}^{T_m} C_{p(S)} \, dT - m\int_{T_m}^{T_2} C_{p(L)} \, dT - \int_{T_1}^{T_2} C_0 \, dT}{m} \quad (6)$$

$$\Delta_m S = \frac{\Delta_m H}{T_m} \quad (7)$$

where Q is the total amount of heat introduced into the sample cell; T_1 is a temperature slightly below T_m; T_2 is a temperature slightly above T_m; $C_{p(S)}$ and $C_{p(L)}$ are the heat capacities of the system in the solid and liquid states, respectively; and C_0 is the heat capacity of the empty cell. The melting enthalpy and entropy were determined to be $\Delta_m H = 9.99$ J g^{-1} and $\Delta_m S = 0.0662$ J K^{-1} g^{-1}, respectively.

Table 3. Thermodynamic Functions of the Unleaded Gasoline 93#

T (K)	C_p (J K^{-1} g^{-1})	$H_{(T)} - H_{(298.15K)}$ (J g^{-1})	$S_{(T)} - S_{(298.15K)}$ (J K^{-1} g^{-1})
100	1.756	−3.393	−0.018
110	1.758	−3.234	−0.017
120	1.762	−3.074	−0.016
130	1.768	−2.914	−0.014
140	1.775	−2.753	−0.013
150	1.784	−2.592	−0.012
160	1.796	−2.429	−0.011
170	1.809	−2.265	−0.010
180	1.823	−2.101	−0.009
190	1.840	−1.934	−0.008
200	1.858	−1.767	−0.007
210	1.879	−1.597	−0.006
220	1.901	−1.425	−0.006
230	1.925	−1.252	−0.005
240	1.950	−1.076	−0.004
250	1.978	−0.898	−0.003
260	2.007	−0.717	−0.003
270	2.039	−0.533	−0.002
280	2.072	−0.347	−0.001
290	2.107	−0.157	−0.001
300	2.143	0.036	0.000
310	2.182	0.232	0.001
320	2.222	0.432	0.001
298.15	2.136	0.000	0.000

3.4. Thermodynamic Function. The thermodynamic function data of the two systems, based on a reference temperature of 298.15 K, in the temperature ranges of 100−320 K for the unleaded gasoline 93# and 100−150 K and 160−320 K for the gasohol were calculated, according to the relationship of heat capacity with the thermodynamic functions.[23] The results of thermodynamic functions $H_{(T)} - H_{(298.15K)}$ and $S_{(T)} - S_{(298.15K)}$ are listed in Tables 3 and 4, respectively.

The values of $S_{(T)} - S_{(298.15K)}$ increase as the temperature increases for the two systems. These values show that the molecules of liquid become more active at higher temperature.

3.5. Excess Thermodynamic Function. Excess thermodynamic properties can be used to investigate the interaction between the compositions in the mixture.

Table 4. Thermodynamic Functions of the Gasohol

T (K)	C_p (J K^{-1} g^{-1})	$H_{(T)} - H_{(298.15K)}$ (J g^{-1})	$S_{(T)} - S_{(298.15K)}$ (J K^{-1} g^{-1})
160	1.909	−3.658	−0.016
170	1.914	−3.416	−0.015
180	1.924	−3.173	−0.013
190	1.939	−2.928	−0.012
200	1.960	−2.681	−0.011
210	1.985	−2.432	−0.010
220	2.016	−2.178	−0.008
230	2.053	−1.921	−0.007
240	2.094	−1.658	−0.006
250	2.141	−1.390	−0.005
260	2.193	−1.116	−0.004
270	2.250	−0.835	−0.003
280	2.312	−0.546	−0.002
290	2.380	−0.249	−0.001
300	2.453	0.057	0.000
310	2.531	0.373	0.001
320	2.615	0.699	0.002
298.15	2.439	0.000	0.000

The excess heat capacity (C_p^E) for the gasohol in the liquid was calculated by the following equation:

$$C_p^E = C_p^{exp} - 0.90C_{p,1}^{id} - 0.10C_{p,2}^{id} \quad (8)$$

where $C_{p,1}^{id}$ and $C_{p,2}^{id}$ are the heat capacities for the unleaded gasoline 93# and ethanol, respectively, and C_p^{exp} is the experimental heat capacity of the gasohol. The values of C_p^{exp}, $C_{p,1}^{id}$, and $C_{p,2}^{id}$ were determined by adiabatic calorimetry. The values of C_p^E are summarized in Table 5. The curve of C_p^E, with respect to T, is given in Figure 5. The values of the excess heat capacities were fitted with the following polynomial expression by the least-squares fitting:

$$C_p^E \text{ (J K}^{-1}\text{ g}^{-1}) = 1.089 \times 10^{-3}T^2 + 1.526 \times 10^{-3}T - 0.4995 \quad (9)$$

where $R^2 = 1$.

The excess thermodynamic functions of the gasohol were derived according to the thermodynamic relationships. The data are given in Table 5.

Figure 5 and Table 5 show that the C_p^E values are all positive for the gasohol in the temperature range of 160−320 K. This means that the interaction between the molecules in the gasohol becomes stronger than that in the unleaded gasoline 93#. This result is in good agreement with the conclusion derived from the differences of the glass-transition temperatures of the ethanol, the unleaded gasoline 93#, and the gasohol.

Table 5. Excess Thermodynamic Functions of the Gasohol

T (K)	C_p^E (J K^{-1} g^{-1})	$H_{(T)}^E - H_{(298.15K)}^E$ (J g^{-1})	$S_{(T)}^E - S_{(298.15K)}^E$ ($\times 10^2$ J K^{-1} g^{-1})
160	0.097	−19.161	−7.449
170	0.092	−18.218	−6.966
180	0.090	−17.313	−6.511
190	0.090	−16.419	−6.075
200	0.094	−15.508	−5.649
210	0.098	−14.553	−5.222
220	0.106	−13.528	−4.786
230	0.118	−12.404	−4.332
240	0.132	−11.155	−3.849
250	0.149	−9.753	−3.328
260	0.169	−8.171	−2.761
270	0.190	−6.382	−2.138
280	0.214	−4.359	−1.449
290	0.242	−2.075	−0.685
300	0.273	0.499	0.164
310	0.305	3.388	1.106
320	0.342	6.620	2.151
298.15	0.267	0.000	0.000

From eq 9, it can be derived that the value of C_p^E reaches the minimum (0.0893 J K^{-1} g^{-1}) at $T = 183.93$ K. The smaller the C_p^E value, the more similar the interaction between the molecules in the system. The solution at the temperature is more similar to the ideal solution. The deviation of the solution from the ideal solution increases as the temperature changes.

4. Conclusion

The glass transitions in the systems of the unleaded gasoline 93# and the gasohol occur at 92.42 and 93.17 K, respectively. For the gasohol, a solid−liquid phase transition occurs at 150.86 K. The interaction between molecules in the gasohol is stronger than that in the unleaded gasoline 93#.

Acknowledgment. This work was financially supported by the National Natural Science Foundation of China (under Contract No. NSFC 20073047) and the K. C. Wong Education Foundation, Hong Kong.

EF030081V